Palmitoylation of the Alphacoronavirus TGEV spike protein S is essential for incorporation into virus-like particles but dispensable for S-M interaction

ARTICLE *in* VIROLOGY · AUGUST 2014

Impact Factor: 3.32 · DOI: 10.1016/j.virol.2014.07.035 · Source: PubMed

5 AUTHORS, INCLUDING:

Bastian Thaa
Karolinska Institutet
22 PUBLICATIONS **215** CITATIONS
SEE PROFILE

Michael Veit
Freie Universität Berlin
92 PUBLICATIONS **1,965** CITATIONS
SEE PROFILE

Virology 464-465 (2014) 397–405

Contents lists available at ScienceDirect

Virology

journal homepage: www.elsevier.com/locate/yviro

Palmitoylation of the *Alphacoronavirus* TGEV spike protein S is essential for incorporation into virus-like particles but dispensable for S–M interaction

Sandra Gelhaus [a], Bastian Thaa [b,1], Kathrin Eschke [a], Michael Veit [b], Christel Schwegmann-Weßels [a,*]

[a] Institute for Virology, Department of Infectious Diseases, University of Veterinary Medicine Hannover, Foundation, Bünteweg 17, 30559 Hannover, Germany
[b] Institute for Virology, Veterinary Faculty, Free University, Robert-von-Ostertag-Str. 7-13, 14163 Berlin, Germany

ARTICLE INFO

Article history:
Received 17 April 2014
Returned to author for revisions
18 May 2014
Accepted 21 July 2014

Keywords:
Coronavirus
TGEV
Alphacoronavirus
Spike protein
Palmitoylation
Cysteine-rich motif
Assembly

ABSTRACT

The spike protein S of coronaviruses contains a highly conserved cytoplasmic cysteine-rich motif adjacent to the transmembrane region. This motif is palmitoylated in the *Betacoronaviruses* MHV and SARS-CoV. Here, we demonstrate by metabolic labeling with [^{3}H]-palmitic acid that the S protein of transmissible gastroenteritis coronavirus (TGEV), an *Alphacoronavirus*, is palmitoylated as well. This is relevant for TGEV replication as virus growth was compromised by the general palmitoylation inhibitor 2-bromopalmitate. Mutation of individual cysteine clusters in the cysteine-rich motif of S revealed that all cysteines must be replaced to abolish acylation and incorporation of S into virus-like particles (VLP). Conversely, the interaction of S with the M protein, essential for VLP incorporation of S, was not impaired by lack of palmitoylation. Thus, palmitoylation of the S protein of *Alphacoronaviruses* is dispensable for S–M interaction, but required for the generation of progeny virions.

Introduction

Coronaviruses (CoVs) are a family of enveloped, single-stranded, positive-sense RNA viruses that have a broad host range, as they infect a wide variety of avian and mammalian species including humans. The family *Coronaviridae* is split up in four genera, the *Alpha-*, *Beta-*, *Delta-* and *Gammacoronavirus.* The genus *Betacoronavirus* comprises the prototype coronavirus mouse hepatitis virus (MHV) as well as the recently emerged human pathogens severe acute respiratory syndrome (SARS)-CoV and middle east respiratory syndrome (MERS)-CoV. The genus *Alphacoronavirus* includes important animal pathogens like feline infectious peritonitis virus (FIPV), porcine epidemic diarrhea virus (PEDV), and transmissible gastroenteritis virus (TGEV), which is the subject of this study. The positive-stranded RNA genome of coronaviruses is associated with the N protein, building up the nucleocapsid, which is surrounded by a lipid bilayer. The structural proteins Spike (S), Membrane (M), and Envelope (E) protein are embedded in this envelope.

Coronaviruses assemble at and bud into intracellular membranes at the endoplasmic reticulum Golgi intermediate compartment, ERGIC (Krijnse-Locker et al., 1994; Tooze et al., 1984). Subcellular targeting signals in the viral proteins direct the proteins towards the budding site (Corse and Machamer, 2002; Lontok et al., 2004; Paul et al., 2014; Schwegmann-Wessels et al., 2004; Swift and Machamer, 1991). Lateral protein interactions between M and M (Locker et al., 1992), M and E (Lim and Liu, 2001), M and N (Narayanan et al., 2000), as well as M and S (Opstelten et al., 1995) proteins play crucial roles during assembly and trigger budding. This paper focuses on the S protein of TGEV. This is a large type 1 membrane protein (250 kDa) that is responsible for the attachment to the cellular receptor and subsequent fusion of viral and cellular membranes. The S protein is incorporated into virus particles by interaction with the M protein (Nguyen and Hogue, 1997; Vennema et al., 1996). This is an indispensable step in the CoV replication cycle to obtain infectious virus particles.

Palmitoylation (S-acylation) is a post-translational modification, in which a saturated fatty acid (most commonly palmitic acid) is linked to a cysteine residue by a thioester bond (Schmidt

* Corresponding author. Tel.: +49 511 9538842; fax: +49 511 9538898.
E-mail address: christel.schwegmann@tiho-hannover.de (C. Schwegmann-Weßels).
[1] Present address: Karolinska Institutet, Department of Microbiology, Tumor and Cell Biology, Nobels väg 16, 171 77 Stockholm, Sweden.

http://dx.doi.org/10.1016/j.virol.2014.07.035
0042-6822/

et al., 1988; Veit et al., 1991). This modification can have effects on protein activity (Huang et al., 2010), transport (Abrami et al., 2008, 2006), and stability (Abrami et al., 2006; Maeda et al., 2010). Most of the cysteines that become acylated are located near the transmembrane region (Veit, 2012; Yang and Compans, 1996; Yik and Weigel, 2002). Palmitoylation of viral proteins has been shown to affect virus assembly or virus replication (Bhattacharya et al., 2004; Gaedigk-Nitschko et al., 1990).

CoV S proteins show a conserved cysteine rich motif (CRM) in the cytoplasmic domain, adjacent to the carboxyterminal end of the transmembrane region (Fig. 1). The CoV S proteins share little sequence homology at this region but the cysteine content is about 35%. For the *Betacoronaviruses* SARS-CoV and MHV, it has been shown that the S proteins are palmitoylated at the CRM (Petit et al., 2007; Thorp et al., 2006). In both viruses the palmitoylation of the S protein is implicitly necessary for the incorporation of the S protein into virus-like particles (VLPs) or virus particles (Thorp et al., 2006; Ujike et al., 2012). However, a partial CRM can be sufficient for the incorporation of the S protein (Ujike et al., 2012; Yang et al., 2012). In contrast to that, the interaction of the S and M proteins has different requirements in both viruses. Treatment with the general palmitoylation inhibitor 2-bromopalmitate disrupted the interaction of S and M proteins in MHV (Thorp et al., 2006). Conversely, the SARS-CoV S–M protein interaction is not impaired with a palmitoylation-null S protein cysteine-mutant (McBride and Machamer, 2010).

These reported findings demonstrate the different requirements in the closely related viruses MHV and SARS-CoV that both belong to the genus *Betacoronavirus*. We wanted to know whether coronaviruses from the genus *Alphacoronavirus* differ from these *Betacoronaviruses* with respect to their role of the S protein's CRM. In our study we addressed the role of the S protein CRM of the *Alphacoronavirus* TGEV during assembly. To this end, we substituted cysteines in the CRM of the TGEV S protein and assessed their effect on VLP formation and on S–M protein interaction. We show that in contrast to the SARS-CoV S protein the TGEV S protein is incorporated into VLPs irrespective of the position of its palmitoylated cysteines. For an efficient interaction between TGEV S and M proteins, palmitoylation of the S protein is not necessary. Our results demonstrate that despite general similarities, coronaviruses show differences regarding the functional role of S protein palmitoylation that may have been induced by evolutionary forces.

Results and discussion

2-BP treatment decreases the infectivity of TGEV

The palmitate analog 2-bromopalmitate (2-BP) inhibits protein palmitoylation in general (Webb et al., 2000). To investigate whether palmitoylation has an impact on TGEV infectivity, we performed a treatment with 2-BP (Fig. 2A). ST cells were infected with TGEV and treated with different concentrations of 2-BP (0, 0.8, 4, 8, and 12 μM). Vesicular stomatitis virus (VSV, grown in BHK-21 cells) was employed as a control since the assembly of this virus does not depend on palmitoylation (Thorp et al., 2006; Whitt and Rose, 1991). These 2-BP concentrations were not cytotoxic for ST cells verified with a WST-1 cell proliferation assay (Fig. 2B). About 24 h after infection, media were harvested and viral infectivity was determined by plaque assay. The production of infectious VSV particles was not significantly inhibited by the 2-BP treatment (Fig. 2A) (Thorp et al., 2006; Whitt and Rose, 1991). In contrast to that, a significant, dose-dependent decrease of TGEV infectivity was observed upon 2-BP treatment. This decrease in infectivity correlated with a decrease in the amount of virus particles in the supernatant of 2-BP-treated, infected cells, as seen by Western blot of pelleted supernatants for viral proteins (Fig. 2C). The amount of protein expression in the cell lysates was not influenced by 2-BP treatment (Fig. 2C). From these results, we conclude that an inhibition of palmitoylation has negative effects on the production of infectious TGEV (but not VSV) particles. While we cannot exclude that the reduction in infectious TGEV particle numbers upon 2-BP treatment is partially caused by inhibited palmitoylation of an essential cellular factor, we considered it most likely that the palmitoylation of a viral protein is required for the production of infectious virions. This led us to assess whether the TGEV S protein is palmitoylated.

TGEV S is palmitoylated in virus particles

Recent studies have shown that the S proteins of MHV and SARS-CoV, both members of the genus *Betacoronavirus*, are palmitoylated (McBride and Machamer, 2010; Petit et al., 2007; Shulla and Gallagher, 2009; Thorp et al., 2006). The cysteine-rich motif (CRM) is highly conserved among CoV S proteins, and a CRM is also found in the S protein of TGEV as a member of the genus *Alphacoronavirus* (Fig. 1). To determine whether the TGEV S protein is also palmitoylated, TGEV was grown in ST cells in the presence of [^{3}H]-palmitic acid to achieve radioactive labeling, followed by pelleting of the virus, SDS-PAGE and fluorography. This revealed that the S protein of TGEV is indeed S-acylated, visible by the band at about 250 kDa which was absent in uninfected cells (Fig. 2D). The specificity of this labeling with [^{3}H]-palmitic acid was confirmed by hydroxylamine treatment (Fig. 2D). Hydroxylamine cleaves thioester linkages at neutral pH and thus any palmitic acid linked to a cysteine residue by S-acylation. The disappearance of the TGEV S protein band after hydroxylamine treatment proves that this protein is S-acylated at at least one cysteine residue.

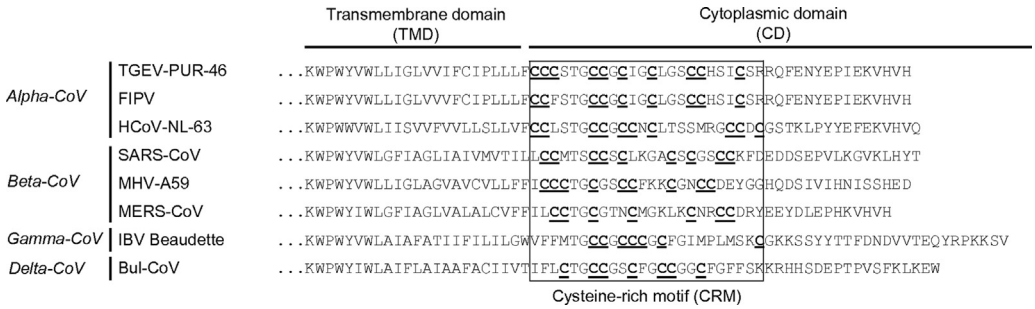

Fig. 1. Sequence alignment of the carboxy-terminal S protein sequences from representative coronavirusspecies. Underlined cysteine residues represent potential palmitoylation sites. TGEV–PUR-46 (transmissible gastroenteritis virus, strain PUR-46), FIPV (feline infectious peritonitis virus), HCoV-NL-63 (human coronavirus NL63), SARS-CoV (severe acute respiratory syndrome coronavirus), MHV-A59 (mouse hepatitis virus, strain A59), MERS-CoV (middle east respiratory syndrome coronavirus), IBV Beaudette (infectious bronchitis virus, strain Beaudette), Bul-CoV (bulbul coronavirus).

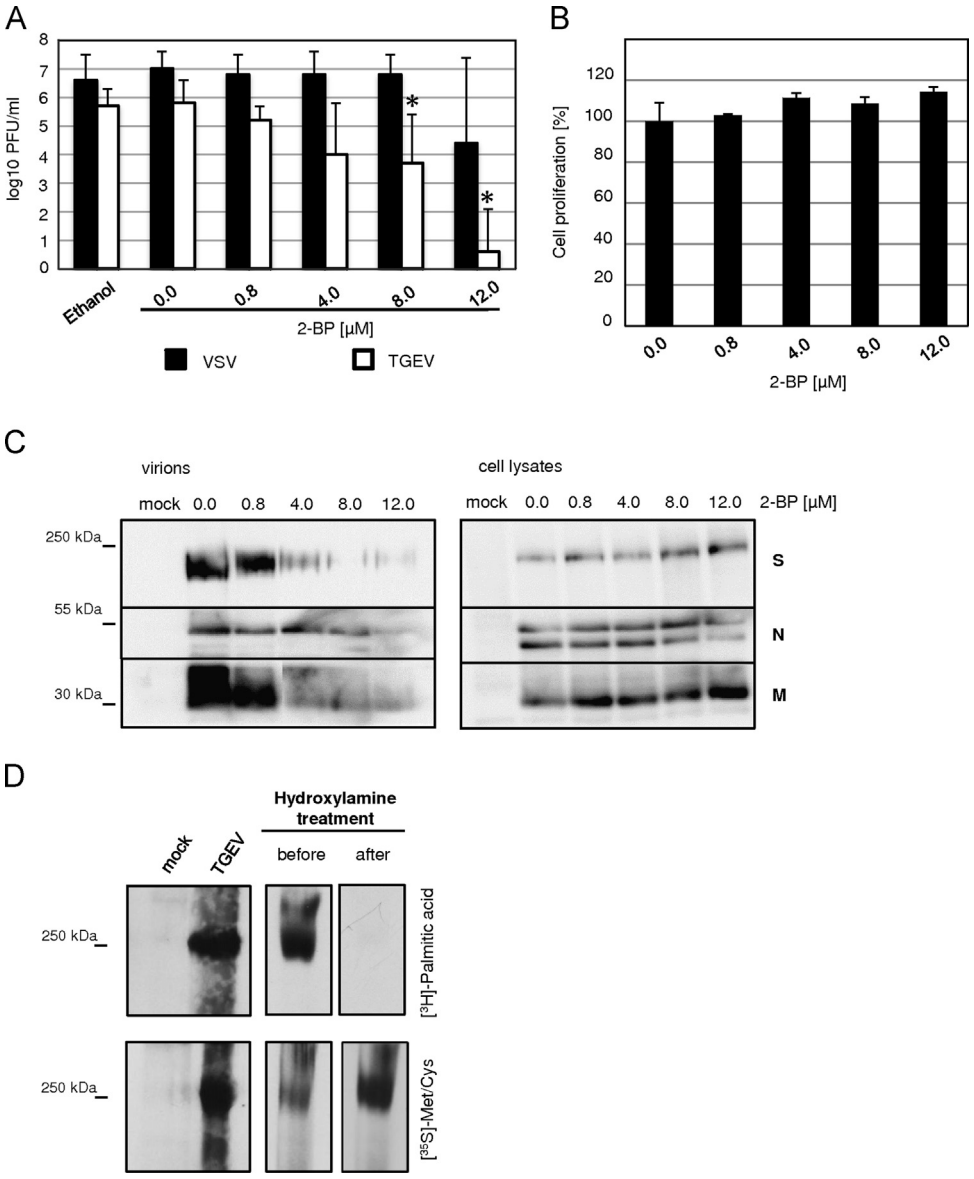

Fig. 2. Palmitoylation of TGEV. (A) Treatment with 2-bromopalmitate (2-BP) decreases the infectivity of TGEV. ST or BHK-21 cells were inoculated with TGEV or VSV, respectively. At 1 h p.i., media were replaced with growth media containing the indicated concentrations of 2-BP or ethanol as 2-BP solvent (ethanol control: amount of ethanol present in the highest 2-BP concentration; 0.0 μM 2-BP: medium without ethanol). Twenty-four hours later, media were collected and the amount of infectious virus particles was determined by plaque assay. Plaque forming units (PFU)/ml are displayed as mean+standard deviation (SD). *, significantly different according to Student's *t* test compared to 0.0 μM 2-BP ($p < 0.05$). (B) 2-BP is not cytotoxic to ST cells at the concentrations used. ST cells were treated with the indicated concentrations of 2-BP and cell proliferation was determined by WST 1-assay. The cell proliferation is indicated as mean+SD in percentage. (C) The amount of viral proteins present in viral particles is reduced after 2-BP treatment. Virions from cell culture supernatants of infected cells, treated with the indicated amounts of 2-BP, were pelleted by ultracentrifugation 24 h p.i. and analyzed by SDS-PAGE and Western blotting (virions). The indicated proteins (S, N, and M) were detected by monoclonal antibodies. The corresponding cells were lysed and the respective proteins were equally analyzed (cell lysates). (D) Palmitoylation of the TGEV S protein in virus particles. Infected and mock-infected ST cells were labeled with [^{3}H]-palmitic acid or [^{35}S]-methionine/cysteine. Radiolabeled virus was analyzed by SDS-PAGE and fluorography. A hydroxylamine treatment was performed to determine the linkage of fatty acids via a thioester bond.

Palmitoylation of TGEV S is necessary for incorporation into VLPs

As the infectivity of TGEV was reduced after 2-BP treatment and the S protein present in TGE virions was shown to be palmitoylated, we concentrated our analysis on the cysteine-rich motif (CRM) present in the cytoplasmic domain of the TGEV S protein (Fig. 1). The Swt protein of the TGEV–PUR-MAD strain contains 10 cysteine residues within the CRM (Sanchez et al., 1990). The CRM of TGEV S can be split up in three cysteine clusters with three to four cysteine residues (Fig. 1). To test whether specific cysteine clusters have a crucial role during virus assembly, partial Cys-mutants were created in addition to the complete cysteine mutant where all cysteines were replaced by alanines (S_C_{1-10}A, Fig. 3A). As the transfection efficiency of ST cells is quite low, BHK-21 cells were transfected with the plasmids encoding for the different Cys-mutants. The labeling with [^{3}H]-palmitic acid showed that all partial mutants were palmitoylated whereas the complete Cys-mutant was not palmitoylated (Fig. 3B). The presence of three cysteines in the CRM (S_C_{1-7}A) was hence sufficient for the protein to be acylated even if the degree of palmitoylation was lower for this mutant (Fig. 3B). It is conceivable that palmitoylation of the CRM cysteines is important for fusion, which is mediated by the S protein. The importance of the CRM of the MHV and SARS-CoV S proteins for fusion has already been proven (Bos et al., 1995; Chang et al., 2000; McBride and Machamer, 2010; Shulla and Gallagher, 2009). In this study, we however evaluated

whether palmitoylation is important for assembly and incorporation of the spike protein into newly generated virus particles. To analyze this role a virus-like particle assay was performed in which the incorporation of S can be analyzed separately from the influence of the fusion capacity of the S protein. The incorporation of the TGEV S protein is an essential step during assembly to form

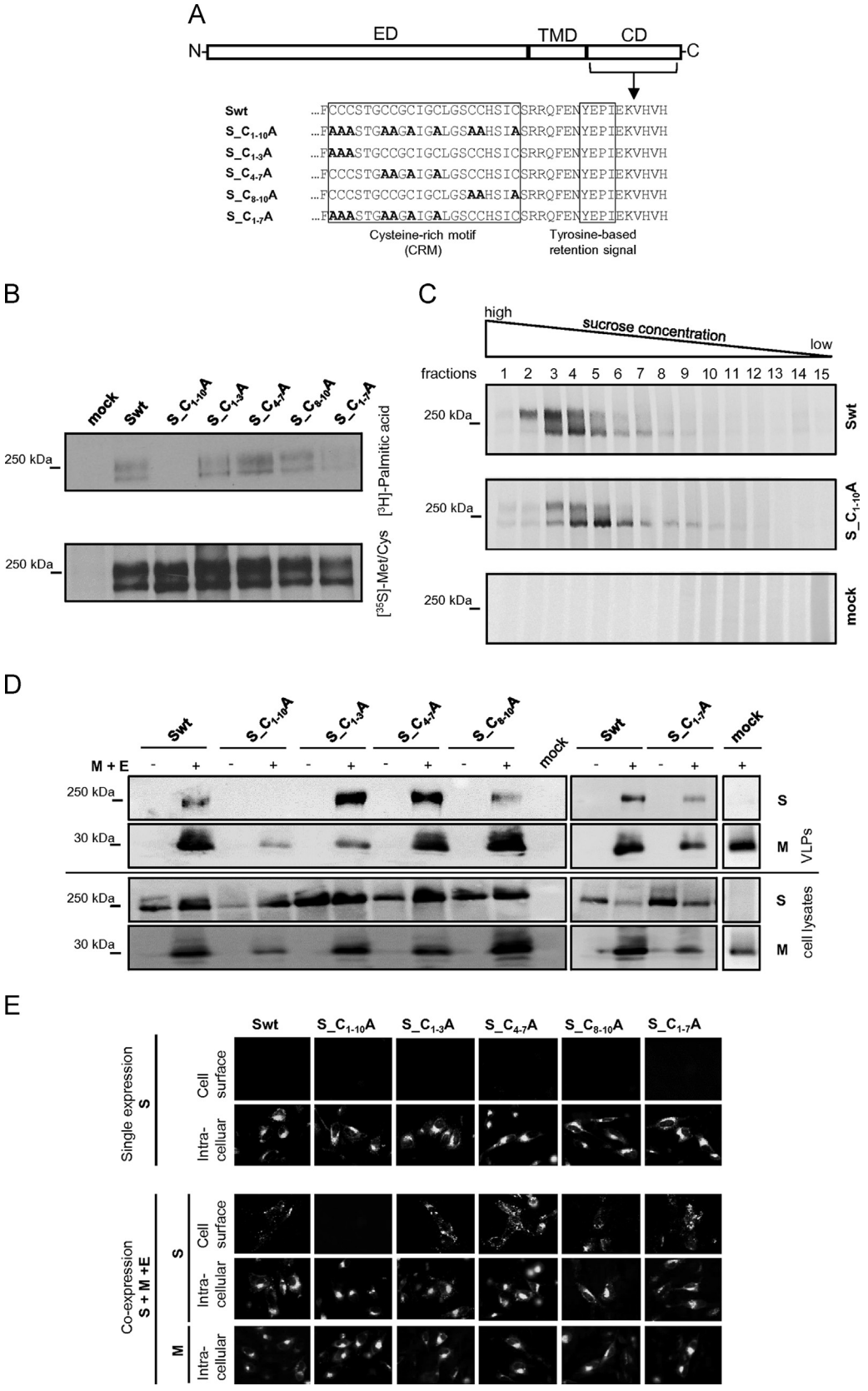

infectious particles. To determine the importance of the TGEV S protein's CRM during virus assembly we analyzed the capability of the TGEV S Cys-mutants to be incorporated into virus-like particles (VLPs, Fig. 3D and E). The co-expression of the TGEV E and M proteins is the minimal requirement for VLP formation (Baudoux et al., 1998). If the S protein is co-expressed with M and E it will be incorporated into VLPs (Vennema et al., 1996). In contrast to the authentic TGEV S protein the complete Cys-mutant S_C_{1-10}A was not incorporated into VLPs (Fig. 3D). The analyzed partial Cys-mutants S_C_{1-3}A, S_C_{4-7}A, S_C_{8-10}A, and S_C_{1-7}A behaved like the TGEV Swt protein and were incorporated into VLPs (Fig. 3D). To confirm these results and to account for variations in protein levels in Western blots, we additionally performed immunofluorescence analysis to show the cell surface transport of S protein (Fig. 3E). We obtained comparable intracellular expression levels of all tested TGEV S proteins and the TGEV M protein. Like in the VLP assay analyzed by Western blot, the S_C_{1-10}A mutant was the only S protein which was not detectable on the cell surface and therefore not incorporated into VLPs (Fig. 3E). These results demonstrate that cysteines are important for the S protein incorporation into viral particles, and that they are at least partially redundant. In contrast to the reports for SARS-CoV (Ujike et al., 2012), the specific position of the cysteine residue inside the cysteine-rich region seems not to be relevant for the incorporation into VLPs. The presence of one cluster of 3 cysteines (S_C_{1-7}A) is enough to incorporate S into VLPs.

The S proteins of coronaviruses are known to form trimers (Delmas and Laude, 1990). To exclude that the inability of the complete Cys-mutant to incorporate into VLPs is caused by a defect in oligomerization, we analyzed the quaternary structure of S_C_{1-10}A with a sucrose density gradient and compared it with the TGEV Swt protein. The results showed that the wild type protein and the Cys-mutant are both detectable in high-concentration sucrose fractions indicating a comparable oligomerization potential (Fig. 3C). In conclusion, the palmitoylation of the TGEV S is necessary for the incorporation of the S protein into VLPs, but does not affect oligomerization of S.

How does palmitoylation of the TGEV S protein influence S incorporation?

One possible explanation might be that the conformation of the cytoplasmic tail of the S protein is crucial for the incorporation of S protein into virus particles. The palmitic acids probably help in membrane attachment of the cytoplasmic tail and may thus define its conformation. This conformation may play a minor role in the binding to the M protein but may be important for the incorporation of the TGEV S protein into virus-like particles. It is possible that the linked fatty acids determine how the protein is positioned in the ERGIC membrane and how it is inserted in the dense matrix formed by the lateral M–M interactions described for coronavirus assembly (de Haan et al., 2000; Neuman et al., 2006).

The palmitoylation of proteins can concentrate them at certain membrane domains (Heakal et al., 2011). A lot of viruses use palmitoylation to target their proteins to lipid microdomains at the plasma membrane for assembly (Bhattacharya et al., 2004; Zhang et al., 2000). Palmitoylated proteins concentrate with interacting proteins at intracellular microdomains as well. As examples, the chaperon Calnexin and the transmembrane thioredoxin protein are recruited to detergent-resistant membranes of the endoplasmic reticulum by palmitoylation (Hayashi and Fujimoto, 2010; Lynes et al., 2012). Thus, a version of the TGEV S protein like the complete Cys-mutant S_C_{1-10}A that lacks palmitic acids may interact with the M protein in an S–M protein co-expression experiment but may not be sorted to the membrane microdomains at the ERGIC in which virus assembly and budding take place and may therefore not be incorporated into newly generated virions or VLPs. McBride and Machamer have shown that the SARS-CoV S protein is present in DRMs at the plasma membrane in single expression experiments. For a complete Cys-mutant of the SARS-CoV S protein it was shown that it is no longer present in DRMs (McBride and Machamer, 2010). These results confirm the hypothesis that the palmitoylation of coronavirus S proteins directs them to membrane microdomains and that this localization is indispensable for the incorporation into VLPs and virions.

Palmitoylation of TGEV S is dispensable for interaction with the M protein

Lateral protein interactions play important roles during virus assembly. The interaction of S and M proteins is essential for the incorporation of S into virus particles. Thus, we aimed to find out whether the palmitoylation of S is required for the interaction with the M protein (as in the case of MHV;(Shulla and Gallagher, 2009; Thorp et al., 2006)), or not (as for SARS-CoV;(McBride and Machamer, 2010; Ujike et al., 2012)). To determine this, we expressed M (with HA-tag) together with the various cysteine mutants of S, with the background of a destroyed ERGIC retention signal (Y/A, Fig. 4A). With this Y/A mutation, S is efficiently transported to the plasma membrane in the absence of M, but is retained intracellularly by M (Fig. 4B and C). Failure of S_Y/A cysteine mutants to interact with M thus leads to plasma membrane delivery of S even in the presence of M. The TGEV S variants depicted in Fig. 4A were expressed in BHK-21 cells by transfection, in the absence or presence of HA-tagged TGEV M. Immunofluorescence analysis was employed to assess the localization of S and M. All partial Cys-mutants and even the complete Cys-mutant showed a similar protein localization pattern with the M protein (Fig. 4B and C). This pattern was identical to the one seen for the S wildtype protein in coexpression with the HA-tagged M protein (S wt, Fig. 4B and C). In contrast to that, the VSV G protein was not retained and not intracellularly clustered by the co-expression of HA-tagged TGEV M protein (VSV G, Fig. 4B and C). These results indicate that specific interactions between the TGEV S and M proteins lead to an intracellular retention of the mutant S proteins and that the interaction of TGEV S and M proteins is not dependent on the palmitoylation of S. Palmitoylation is known to affect protein trafficking (Greaves and Chamberlain, 2007; Resh, 1999, 2006). Our results show that this is not the case for the TGEV S since the full cysteine-mutant with

Fig. 3. Palmitoylation of S is necessary for incorporation into VLPs. (A) Schematic illustration of TGEV S wild-type and TGEV S cysteine-mutants. The cysteine-rich motif (CRM) and the tyrosine-based retention signal are highlighted by boxes. Cysteines substituted by alanines are written in bold. ED, ectodomain; TMD, transmembrane domain; CD, cytoplasmic domain. (B) The complete TGEV S cysteine-mutant is not palmitoylated, whereas the partial cysteine-mutants are. BHK-21 cells expressing TGEV Swt or the indicated TGEV S cysteine-mutants were labeled with [^{3}H]-palmitic acid or [^{35}S]-methionine/cysteine for 5 h. The cells were lysed and S protein was immunoprecipitated and subjected to SDS-PAGE and fluorography. (C) Lack of cysteines in the CRM does not affect oligomerization. BHK-21 cells expressing TGEV Swt or S_C_{1-10}A were labeled with [^{35}S]-methionine/cysteine for 6 h, then solubilized in 6 mM dodecyl-β-*m*-maltoside. A sucrose density gradient was overlaid with these cell lysates and was ultracentrifuged. Fractions were collected, immunoprecipitated, and subjected to SDS-PAGE and phosphorimaging. (D) TGEV Swt and partial TGEV S cysteine-mutants can be incorporated into VLPs, whereas a complete TGEV S cysteine-mutant cannot. BHK-21 cells were transfected with expression plasmids for the indicated versions of TGEV S, and for TGEV M and E proteins (+) or a mock expression plasmid (−). At 24 h p.t., VLPs were collected by ultracentrifugation through a sucrose cushion, and analyzed by SDS-PAGE and Western blotting. The corresponding cell lysates were checked for the presence of the respective proteins. (E) The TGEV S protein is detectable on the cell surface of BHK-21 cells after co-expression of S, M, and E proteins. BHK-21 cells were transfected with expression plasmids for the indicated versions of TGEV S alone or together with TGEV M and E encoding plasmids. At 24 h p.t., the S protein expression was detected by cell surface immunostaining or staining after permeabilization of the cells. In addition to the TGEV S protein the TGEV M protein was detected intracellularly in the parallel co-expression experiment.

Y/A-mutation traffics correctly to the cell surface in single expression (Fig. 4C) and the full cysteine-mutant has a comparable oligomerization potential as the wildtype protein (Fig. 3C).

Studies on MHV showed that the cytoplasmic tail of the S protein and, more specifically, the membrane adjacent cysteine-rich region is important for the interaction with M and for

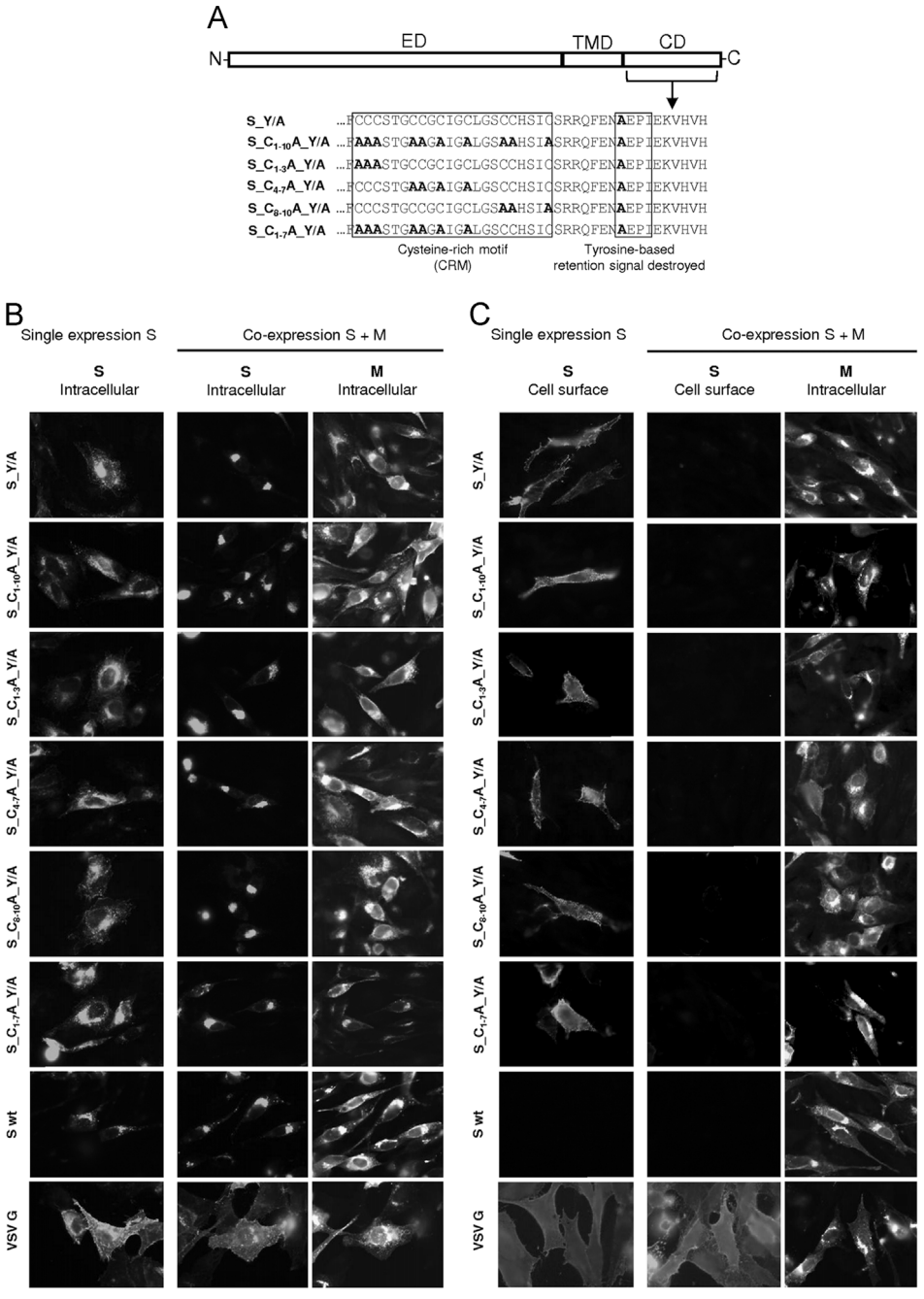

D

	Betacoronavirus		Alphacoronavirus
	MHV	**SARS-CoV**	**TGEV**
S-M protein interaction	palmitoylation dependent *(Thorp et al., 2006; Shulla et al., 2009)*	**not palmitoylation dependent** *(McBride and Machamer, 2010; Ujike et al., 2012)*	**not palmitoylation dependent**
S protein incorporation	**palmitoylation dependent** *(Thorp et al., 2006; Shulla et al., 2009)*	**palmitoylation dependent** *(Ujike et al., 2012)*	**palmitoylation dependent**
	no specific cysteine-cluster *(Yang et al., 2012)* the C-terminal cysteine-cluster *(Shulla et al., 2009)*	the C-terminal cysteine-cluster *(Ujike et al., 2012)*	**no specific cysteine-cluster**

incorporation into virus-like particles (Bosch et al., 2005; Godeke et al., 2000). Our results for TGEV are similar to the published results for the SARS-CoV S protein, where the cysteine-rich motif is not important for the interaction between S and M proteins (McBride and Machamer, 2010). For these coronaviral spike proteins other parts like the transmembrane domain or the ectodomain of S could play a role in the interaction with the M protein.

Conclusion

It is of significant interest to understand how the S protein is incorporated into coronavirus particles because the S protein mediates binding to the cellular receptor and fusion with the cellular membrane and is therefore indispensable for the generation of infectious virus particles. One important result from our study is that the palmitoylation of the cysteine-rich motif at the carboxy-terminus of the TGEV S protein is necessary for the incorporation of S into virus-like particles. Furthermore, our results suggest that the loss of palmitoylation does not affect the interaction with the TGEV M protein. Here, we show that for TGEV, the interaction of the S protein with M has different requirements than the incorporation of S into virus particles.

This is the first study about the role of palmitoylation in virus assembly for the genus *Alphacoronavirus* in the family *Coronaviridae*, demonstrating that there are some similarities but also differences in the requirements for coronavirus assembly in MHV (Shulla and Gallagher, 2009; Thorp et al., 2006; Yang et al., 2012), SARS-CoV (McBride and Machamer, 2010; Ujike et al., 2012), and the *Alphacoronavirus* TGEV (Fig. 4D).

Future studies about the role of palmitoylation of the TGEV S protein in virus assembly should include the analysis of recombinant virions that contain the respective cysteine mutations. Additionally it should be analyzed if the TGEV S protein is directed to distinct membrane microdomains inside the ERGIC and if this localization is determined by cysteine palmitoylation.

Materials and methods

Cells

BHK-21 cells were grown in Eagle's minimal essential medium (EMEM; Gibco BRL) supplemented with 5% fetal calf serum (FCS; Biochrom). ST (swine testicular) cells were propagated in Dulbecco's minimal essential medium (DMEM; Gibco BRL) containing 10% Mycoplex fetal bovine serum (GE Healthcare).

Plasmid DNAs, construction of plasmids

The TGEV S gene, strain PUR-46-MAD (Sanchez et al., 1990), was cloned into the pCG1 plasmid using *Bam*HI and *Pst*I restriction sites (Cathomen et al., 1995; Schwegmann-Wessels et al., 2006). Cysteine mutants of TGEV S protein and TGEV S_Y/A protein were generated by a standard hybridization PCR technique, as described previously (Schwegmann-Wessels et al., 2004). The generated cysteine mutant proteins are illustrated in Figs. 3A and 4A. An HA-peptide (MYPYDVPDYA) was C-terminally fused to the TGEV M protein using standard PCR techniques. The mutated gene regions generated by PCR were verified by sequencing (Eurofins MWG Operon).

Transient transfections (PEI and Lipofectamine)

Transfection of BHK-21 cells in 6- and 24-well-plates was performed by using Lipofectamine 2000 reagent (Life Technologies) following the manufacturer's instructions. BHK-21 cells in 10 cm-diameter dishes were transfected by using Polyethylenimine (PEI; Polysciences). Transfections were carried out at a confluency of 70–80%. The medium was replaced with 7 ml fresh EMEM containing 3% FCS. A total of 12 μg DNA were pipetted in 3 ml Opti-MEM (Life Technologies) and were incubated for 5 min. Then, 20 μl of a 1 μg/μl PEI-working solution was added. The mixture was incubated for 15 min at room temperature and added to the cells.

2-bromopalmitate treatment and plaque assay

TGEV was propagated on ST cells and VSV (strain Indiana) on BHK-21 cells. Infections were carried out on confluent monolayers with an MOI of 0.001 at 37 °C on a rocking shaker. At 1 h p.i. media were removed and cells rinsed with PBS to prepare for further treatments. For 2-bromopalmitate (2-BP) treatment infected cells were grown in DMEM containing variable amounts of 2-BP (0, 0.8, 4, 8, and 12 μM) or ethanol (solvent of 2-BP). At a detectable cytopathic effect supernatants were harvested and spun at 2800*g* for 10 min at 4 °C to remove cellular debris. The amount of infectious virus particles was determined by plaque assay as described by Krempl et al. (2000) using ST cells (TGEV) or BHK-21 cells (VSV). The cytotoxicity of the 2-BP treatment on ST cells was quantified with the cell proliferation reagent WST-1 (Roche) in 96-well microplates according to the manufacturer's instructions. Viral proteins (S, M, and N) incorporated into virions were detected via SDS-PAGE and Western blot analysis after ultracentrifugation of the respective cell culture supernatants. S protein was detected with mAB 6A.C3 (1:200), N protein with anti-coronavirus monoclonal antibody FIPV3-70 (1:1000, Thermo Scientific), and M protein with mAB 9D.B4 (1:200) followed by incubation with an anti-mouse peroxidase-conjugated antibody (Dako; 1:1000). Protein expression in the cells was equally detected after cell lysis.

Labeling of viral particles with [^{3}H]-palmitic acid

ST cells in 15 cm-diameter dishes were mock-infected or infected with TGEV at an MOI of 10. At 3 h p.i. the cells were labeled with 20 μCi/ml [^{3}H]-palmitic acid ([9,10-^{3}H(N)], Perkin-Elmer) or [^{35}S]-Met/Cys (EasyTagExpress mix, Perkin-Elmer) in Met/Cys-free Dulbecco's modified Eagle's medium (DMEM; PAN Biotech) supplemented with 5 mM L-glutamine (PAN Biotech). At 24 h p.i supernatants were harvested and cleared by low-speed centrifugation (3000g, 20 min, 4 °C) followed by pelleting of the virus by ultracentrifugation in an SW28m rotor (Beckman Coulter) at 28,000 rpm for 2 h at 4 °C. The pellet was resuspended in 2 ×

Fig. 4. Palmitoylation of TGEV S is dispensable for interaction with the M protein. (A) Schematic illustration of TGEV S_Y/A and TGEV S cysteine-mutants with Y/A-mutations. The cysteine-rich motif (CRM) and the destroyed tyrosine-based retention signal are highlighted. Substitutions by alanine are written in bold. ED, ectodomain; TMD, transmembrane domain; CD, cytoplasmic domain. (B) Every TGEV S cysteine-mutant shows an intracellular clustering in co-expression with the HA-tagged TGEV M protein. BHK-21 cells expressing either the S proteins alone (mutants shown in A, S wt, or VSV G) or in co-expression with the TGEV M protein were permeabilized with Triton-X 100 prior to antibody incubation. The same field is shown in each set of images for the coexpression of S and M. (C) Every TGEV S cysteine-mutant is retained intracellularly when co-expressed with the HA-tagged TGEV M protein. The S protein (or the VSV G protein) was detected on the cell surface of non-permeabilized BHK-21 cells expressing either the S proteins alone or in co-expression with the TGEV M. The detection of the HA-tagged TGEV M protein was done after permeabilization with Triton-X 100 prior to antibody incubation. The same field is shown for the detection of surface-expressed S together with the total M staining. (D) Comparison of the role of coronaviral S protein palmitoylation for MHV (references indicated), SARS-CoV (references indicated), and TGEV (this study) for S–M protein interaction and S incorporation into VLPs or virions.

non-reducing SDS sample buffer (0.1 M Tris–HCl, 2% SDS, 20% glycerol, 2% bromophenol blue) and analyzed by SDS-PAGE and fluorography, as described previously (Thaa et al., 2011). To determine an ester-type linkage of the acylated viral protein a hydroxylamine treatment under neutral pH conditions was performed, as described previously (Veit et al., 2008).

Metabolic labeling with [^{3}H]-palmitic acid and immunoprecipitation

BHK-21 cells grown in 6-well-plates were transfected with TGEV S expression plasmids using Lipofectamine 2000. Twenty-four hours post-transfection, cells were washed with phosphate-buffered saline (PBS) and incubated for 1 h in Met/Cys-free DMEM supplemented with 5 mM L-glutamine. Subsequently, cells were labeled for 5 or 19 h with 1000 μCi/ml [^{3}H]-palmitic acid. A parallel dish was labeled with 600 μCi/ml [^{35}S]-Met/Cys. Cells were lysed in NP-40 lysis buffer (0.5% sodium deoxycholate, 1% Nonidet P40, 150 mM NaCl, 50 mM Tris–HCl, pH 7.5) containing protease inhibitor (Complete, Roche) for 30 min at 4 °C. Lysates were clarified for 30 min at 20,000*g*, 4 °C. S protein was immunoprecipitated with mouse anti-TGEV S monoclonal antibody, 6A.C3 (Gebauer et al., 1991) and protein A-sepharose (Sigma) overnight at 4 °C. Immunoprecipitates were washed three times with NP-40 lysis buffer and were eluted in 2 × non-reducing SDS sample buffer at 96 °C for 10 min followed by SDS-PAGE and fluorography.

Indirect immunofluorescence microscopy

BHK-21 cells grown on coverslips in 24-well-plates were co-transfected with pCG1-TGEV-S wt, pCG1-TGEV-S_Y/A, pCG1-TGEV-Cys-mutants, pCG1-VSV-G with empty vector (pCG1) or with HA-tagged pCG1-TGEV-M. The transfection ratio of S to M was 5:1. At 18 h p.t. cells were fixed with 3% paraformaldehyde in PBS and indirect immunofluorescence analysis was performed. For intracellular protein detection cells were permeabilized with 0.2% Triton/PBS for 5 min. Detection of TGEV S protein was performed as described previously (Schwegmann-Wessels et al., 2004). The VSV G protein was detected with the monoclonal antibodies I-1 and I-14 (Hanika et al., 2005). As secondary antibody, a Cy3-conjugated sheep–anti-mouse antibody (1:300, Sigma) was used. The HA-tagged TGEV M was visualized by an anti-HA-tag antibody (rabbit, 1:200, Sigma) and anti-rabbit fluorescein isothiocyanate (FITC)-labeled secondary antibody (goat anti-rabbit, 1:300, Sigma). Fluorescence micrographs were acquired on a Nikon Eclipse Ti microscope. For the detection of S protein present in VLPs on the cell surface plasmids encoding for the respective S proteins were co-transfected with TGEV M and E plasmids. The immunostaining was performed as described above with and without permeabilization of the cells.

VLP-assay

BHK-21 cells grown in 10 cm-diameter dishes were co-transfected with plasmids (pCG1) encoding the TGEV M, E and S proteins. At 24 h p.t. VLPs secreted into the culture medium were purified through a 25% sucrose cushion by ultracentrifugation at 35,000 rpm in an SW 41 rotor (Beckman Coulter) for 1 h at 4 °C. VLP pellets were solubilized in 50 μl 2 × SDS sample puffer and subjected to SDS-PAGE. Cells were lysed in NP-40 lysis puffer and were also subjected to SDS-PAGE. SDS gels were transferred by a semi-dry technique (Kyhse-Andersen, 1984) to nitrocellulose membranes (GE Healthcare) that were subsequently blocked overnight with 1% blocking reagent (Roche) in blocking buffer (100 mM maleic acid, 150 mM NaCl, pH 7.5). S protein was detected with mAB 6A.C3 (1:200) and M protein with mAB 9D.B4 (1:200) followed by incubation with an anti-mouse peroxidase-conjugated antibody (Dako; 1:1000). The nitrocellulose membrane was incubated with a chemiluminescent peroxidase substrate (Thermo Scientific), and chemiluminescence was measured with a Chemi Doc system (Biorad).

Cell lysate fractionation on sucrose density gradients

BHK-21 cells were seeded in 10 cm-diameter dishes and were transfected with pCG1-TGEV-Swt, pCG1-TGEV-S_C$_{1-10}$A or empty vector (pCG1) one day later. At 24 h p.t. the cells were metabolically labeled with 100 μCi/ml [^{35}S]-Met/Cys in methionine- and cysteine-free Dulbecco's modified Eagle's medium (Gibco) supplemented with 4 mM L-glutamine (PAA Laboratories) for 6 h. The cells were solubilized in 250 μl 6 mM dodecyl-β-*m*-maltoside (Sigma), 10 mM Tris, 150 mM NaCl, pH 7.5, and protease inhibitors (Complete; Roche) per dish. The cell lysates were homogenized by a needle (G21 × 1, 5″) and lysed for 3 h at 4 °C. One milliliter of the cell lysate was loaded onto a sucrose gradient that consisted of a 50%-sucrose-cushion at the bottom of the tube overlaid with a gradient of 10–30% sucrose (in 10 mM Tris, 150 mM NaCl, pH 7.5, 6 mM dodecyl-β-*m*-maltoside, and protease inhibitor). The gradient was centrifuged at 35,000 rpm for 18 h in an SW40 Ti rotor at 4 °C (Beckman Coulter) and then divided into 700 μl fractions. 700 μl NP-40 lysis buffer was added and S proteins were isolated by immunoprecipitation. The radioactively labeled proteins were analyzed in SDS-PAGE and were visualized by phosphorimaging (Molecular Imager FX phosphoimager; Biorad).

Acknowledgments

Financial support was provided by a grant to C.S.-W. (SCHW 1408/1.1) and to M.V. (Ve 141/10.1) from the German Research Foundation (DFG). C.S.-W. is funded by the Emmy Noether Programme from the DFG.

This work was performed by S.G. in partial fulfillment of the requirements for the PhD degree from the University of Veterinary Medicine Hannover. We thank Sandra Bauer for technical assistance.

We thank L. Enjuanes for the monoclonal antibodies 6A.C3 against the TGEV S protein and 9D.B4 against the TGEV M protein. We thank R. Cattaneo for providing the pCG1 expression plasmid.

References

Abrami, L., Kunz, B., Iacovache, I., van der Goot, F.G., 2008. Palmitoylation and ubiquitination regulate exit of the Wnt signaling protein LRP6 from the endoplasmic reticulum. Proc. Natl. Acad. Sci. USA 105 (14), 5384–5389.

Abrami, L., Leppla, S.H., van der Goot, F.G., 2006. Receptor palmitoylation and ubiquitination regulate anthrax toxin endocytosis. J. Cell Biol. 172 (2), 309–320.

Baudoux, P., Carrat, C., Besnardeau, L., Charley, B., Laude, H., 1998. Coronavirus pseudoparticles formed with recombinant M and E proteins induce alpha interferon synthesis by leukocytes. J. Virol. 72 (11), 8636–8643.

Bhattacharya, J., Peters, P.J., Clapham, P.R., 2004. Human immunodeficiency virus type 1 envelope glycoproteins that lack cytoplasmic domain cysteines: impact on association with membrane lipid rafts and incorporation onto budding virus particles. J. Virol. 78 (10), 5500–5506.

Bos, E.C.W., Heunen, L., Luytjes, W., Spaan, W.J.M., 1995. Mutational analysis of the murine coronavirus spike protein: effect on cell-to-cell fusion. Virology 214 (2), 453–463.

Bosch, B.J., de Haan, C.A., Smits, S.L., Rottier, J., 2005. Spike protein assembly into the coronavirion: exploring the limits of its sequence requirements. Virology 334 (2), 306–318.

Cathomen, T., Buchholz, C.J., Spielhofer, P., Cattaneo, R., 1995. Preferential initiation at the second AUG of the measles virus F mRNA: a role for the long untranslated region. Virology 214 (2), 628–632.

Chang, K.W., Sheng, Y.W., Gombold, J.L., 2000. Coronavirus-induced membrane fusion requires the cysteine-rich domain in the spike protein. Virology 269 (1), 212–224.

Corse, E., Machamer, C.E., 2002. The cytoplasmic tail of infectious bronchitis virus E protein directs Golgi targeting. J. Virol. 76 (3), 1273–1284.

de Haan, C.A., Vennema, H., Rottier, P.J., 2000. Assembly of the coronavirus envelope: homotypic interactions between the M proteins. J. Virol. 74 (11), 4967–4978.
Delmas, B., Laude, H., 1990. Assembly of coronavirus spike protein into trimers and its role in epitope expression. J. Virol. 64 (11), 5367–5375.
Gaedigk-Nitschko, K., Ding, M.X., Levy, M.A., Schlesinger, M.J., 1990. Site-directed mutations in the Sindbis virus 6K protein reveal sites for fatty acylation and the underacylated protein affects virus release and virion structure. Virology 175 (1), 282–291.
Gebauer, F., Posthumus, W.P., Correa, I., Sune, C., Smerdou, C., Sanchez, C.M., Lenstra, J.A., Meloen, R.H., Enjuanes, L., 1991. Residues involved in the antigenic sites of transmissible gastroenteritis coronavirus S glycoprotein. Virology 183 (1), 225–238.
Godeke, G.J., de Haan, C.A., Rossen, J.W., Vennema, H., Rottier, P.J., 2000. Assembly of spikes into coronavirus particles is mediated by the carboxy-terminal domain of the spike protein. J. Virol. 74 (3), 1566–1571.
Greaves, J., Chamberlain, L.H., 2007. Palmitoylation-dependent protein sorting. J. Cell Biol. 176 (3), 249–254.
Hanika, A., Larisch, B., Steinmann, E., Schwegmann-Wessels, C., Herrler, G., Zimmer, G., 2005. Use of influenza C virus glycoprotein HEF for generation of vesicular stomatitis virus pseudotypes. J. Gen. Virol. 86 (Pt 5), 1455–1465.
Hayashi, T., Fujimoto, M., 2010. Detergent-resistant microdomains determine the localization of sigma-1 receptors to the endoplasmic reticulum–mitochondria junction. Mol. Pharmacol. 77 (4), 517–528.
Heakal, Y., Woll, M.P., Fox, T., Seaton, K., Levenson, R., Kester, M., 2011. Neurotensin receptor-1 inducible palmitoylation is required for efficient receptor-mediated mitogenic-signaling within structured membrane microdomains. Cancer Biol. Ther. 12 (5), 427–435.
Huang, K., Kang, M.H., Askew, C., Kang, R., Sanders, S.S., Wan, J., Davis, N.G., Hayden, M.R., 2010. Palmitoylation and function of glial glutamate transporter-1 is reduced in the YAC128 mouse model of Huntington disease. Neurobiol. Dis. 40 (1), 207–215.
Krempl, C., Ballesteros, M.L., Zimmer, G., Enjuanes, L., Klenk, H.D., Herrler, G., 2000. Characterization of the sialic acid binding activity of transmissible gastroenteritis coronavirus by analysis of haemagglutination-deficient mutants. J. Gen. Virol. 81 (Pt 2), 489–496.
Krijnse-Locker, J., Ericsson, M., Rottier, P.J., Griffiths, G., 1994. Characterization of the budding compartment of mouse hepatitis virus: evidence that transport from the RER to the Golgi complex requires only one vesicular transport step. J. Cell Biol. 124 (1–2), 55–70.
Kyhse-Andersen, J., 1984. Electroblotting of multiple gels: a simple apparatus without buffer tank for rapid transfer of proteins from polyacrylamide to nitrocellulose. J. Biochem. Biophys. Methods 10 (3–4), 203–209.
Lim, K.P., Liu, D.X., 2001. The missing link in coronavirus assembly. Retention of the avian coronavirus infectious bronchitis virus envelope protein in the pre-Golgi compartments and physical interaction between the envelope and membrane proteins. J. Biol. Chem. 276 (20), 17515–17523.
Locker, J.K., Rose, J.K., Horzinek, M.C., Rottier, P.J., 1992. Membrane assembly of the triple-spanning coronavirus M protein. Individual transmembrane domains show preferred orientation. J. Biol. Chem. 267 (30), 21911–21918.
Lontok, E., Corse, E., Machamer, C.E., 2004. Intracellular targeting signals contribute to localization of coronavirus spike proteins near the virus assembly site. J. Virol. 78 (11), 5913–5922.
Lynes, E.M., Bui, M., Yap, M.C., Benson, M.D., Schneider, B., Ellgaard, L., Berthiaume, L.G., Simmen, T., 2012. Palmitoylated TMX and calnexin target to the mitochondria-associated membrane. EMBO J. 31 (2), 457–470.
Maeda, A., Okano, K., Park, P.S., Lem, J., Crouch, R.K., Maeda, T., Palczewski, K., 2010. Palmitoylation stabilizes unliganded rod opsin. Proc. Natl. Acad. Sci. USA 107 (18), 8428–8433.
McBride, C.E., Machamer, C.E., 2010. Palmitoylation of SARS-CoV S protein is necessary for partitioning into detergent-resistant membranes and cell–cell fusion but not interaction with M protein. Virology 405 (1), 139–148.
Narayanan, K., Maeda, A., Maeda, J., Makino, S., 2000. Characterization of the coronavirus M protein and nucleocapsid interaction in infected cells. J. Virol. 74 (17), 8127–8134.
Neuman, B.W., Adair, B.D., Yoshioka, C., Quispe, J.D., Orca, G., Kuhn, P., Milligan, R.A., Yeager, M., Buchmeier, M.J., 2006. Supramolecular architecture of severe acute respiratory syndrome coronavirus revealed by electron cryomicroscopy. J. Virol. 80 (16), 7918–7928.
Nguyen, V.P., Hogue, B.G., 1997. Protein interactions during coronavirus assembly. J. Virol. 71 (12), 9278–9284.
Opstelten, D.J., Raamsman, M.J., Wolfs, K., Horzinek, M.C., Rottier, P.J., 1995. Envelope glycoprotein interactions in coronavirus assembly. J. Cell Biol. 131 (2), 339–349.
Paul, A., Trincone, A., Siewert, S., Herrler, G., Schwegmann-Wessels, C., 2014. A lysine–methionine exchange in a coronavirus surface protein transforms a retention motif into an endocytosis signal. Biol. Chem. 395 (6), 657–665.
Petit, C.M., Chouljenko, V.N., Iyer, A., Colgrove, R., Farzan, M., Knipe, D.M., Kousoulas, K.G., 2007. Palmitoylation of the cysteine-rich endodomain of the SARS-coronavirus spike glycoprotein is important for spike-mediated cell fusion. Virology 360 (2), 264–274.
Resh, M.D., 1999. Fatty acylation of proteins: new insights into membrane targeting of myristoylated and palmitoylated proteins. Biochim. Biophys. Acta 1451 (1), 1–16.
Resh, M.D., 2006. Trafficking and signaling by fatty-acylated and prenylated proteins. Nat. Chem. Biol. 2 (11), 584–590.
Sanchez, C.M., Jimenez, G., Laviada, M.D., Correa, I., Sune, C., Bullido, M.J., Gebauer, F., Smerdou, C., Callebaut, P., Escribano, J.M., Enjuanes, L., 1990. Antigenic homology among coronaviruses related to transmissible gastroenteritis virus. Virology 174 (2), 410–417.
Schmidt, M., Schmidt, M.F., Rott, R., 1988. Chemical identification of cysteine as palmitoylation site in a transmembrane protein (Semliki Forest virus E1). J. Biol. Chem. 263 (35), 18635–18639.
Schwegmann-Wessels, C., Al-Falah, M., Escors, D., Wang, Z., Zimmer, G., Deng, H., Enjuanes, L., Naim, H.Y., Herrler, G., 2004. A novel sorting signal for intracellular localization is present in the S protein of a porcine coronavirus but absent from severe acute respiratory syndrome-associated coronavirus. J. Biol. Chem. 279 (42), 43661–43666.
Schwegmann-Wessels, C., Ren, X., Herrler, G., 2006. Intracellular transport of the S proteins of coronaviruses. Adv. Exp. Med. Biol. 581, 271–275.
Shulla, A., Gallagher, T., 2009. Role of spike protein endodomains in regulating coronavirus entry. J. Biol. Chem. 284 (47), 32725–32734.
Swift, A.M., Machamer, C.E., 1991. A Golgi retention signal in a membrane-spanning domain of coronavirus E1 protein. J. Cell Biol. 115 (1), 19–30.
Thaa, B., Levental, I., Herrmann, A., Veit, M., 2011. Intrinsic membrane association of the cytoplasmic tail of influenza virus M2 protein and lateral membrane sorting regulated by cholesterol binding and palmitoylation. Biochem. J. 437, 389–397.
Thorp, E.B., Boscarino, J.A., Logan, H.L., Goletz, J.T., Gallagher, T.M., 2006. Palmitoylations on murine coronavirus spike proteins are essential for virion assembly and infectivity. J. Virol. 80 (3), 1280–1289.
Tooze, J., Tooze, S., Warren, G., 1984. Replication of coronavirus MHV-A59 in sac- cells: determination of the first site of budding of progeny virions. Eur. J. Cell Biol. 33 (2), 281–293.
Ujike, M., Huang, C., Shirato, K., Matsuyama, S., Makino, S., Taguchi, F., 2012. Two palmitylated cysteine residues of the severe acute respiratory syndrome coronavirus spike (S) protein are critical for S incorporation into virus-like particles, but not for M-S co-localization. J. Gen. Virol. 93 (Pt 4), 823–828.
Veit, M., 2012. Palmitoylation of virus proteins. Biol. Cell 104 (9), 493–515.
Veit, M., Klenk, H.D., Kendal, A., Rott, R., 1991. The M2 protein of influenza A virus is acylated. J. Gen. Virol. 72 (Pt 6), 1461–1465.
Veit, M., Ponimaskin, E., Schmidt, M.F., 2008. Analysis of S-acylation of proteins. Methods Mol. Biol. 446, 163–182.
Vennema, H., Godeke, G.J., Rossen, J.W., Voorhout, W.F., Horzinek, M.C., Opstelten, D.J., Rottier, P.J., 1996. Nucleocapsid-independent assembly of coronavirus-like particles by co-expression of viral envelope protein genes. EMBO J. 15 (8), 2020–2028.
Webb, Y., Hermida-Matsumoto, L., Resh, M.D., 2000. Inhibition of protein palmitoylation, raft localization, and T cell signaling by 2-bromopalmitate and polyunsaturated fatty acids. J. Biol. Chem. 275 (1), 261–270.
Whitt, M.A., Rose, J.K., 1991. Fatty acid acylation is not required for membrane fusion activity or glycoprotein assembly into VSV virions. Virology 185 (2), 875–878.
Yang, C., Compans, R.W., 1996. Palmitoylation of the murine leukemia virus envelope glycoprotein transmembrane subunits. Virology 221 (1), 87–97.
Yang, J., Lv, J., Wang, Y., Gao, S., Yao, Q., Qu, D., Ye, R., 2012. Replication of murine coronavirus requires multiple cysteines in the endodomain of spike protein. Virology 427 (2), 98–106.
Yik, J.H., Weigel, P.H., 2002. The position of cysteine relative to the transmembrane domain is critical for palmitoylation of H1, the major subunit of the human asialoglycoprotein receptor. J. Biol. Chem. 277 (49), 47305–47312.
Zhang, J., Pekosz, A., Lamb, R.A., 2000. Influenza virus assembly and lipid raft microdomains: a role for the cytoplasmic tails of the spike glycoproteins. J. Virol. 74 (10), 4634–4644.